Atherosclerosis 275 (2018) 43–49

Contents lists available at ScienceDirect

Atherosclerosis

journal homepage: www.elsevier.com/locate/atherosclerosis

Therapeutic silencing of FSP27 reduces the progression of atherosclerosis in *Ldlr*$^{-/-}$ mice

Ananthi Rajamoorthi [a], Richard G. Lee [b], Ángel Baldán [a, c, d, *]

[a] Edward A. Doisy Department of Biochemistry & Molecular Biology, Saint Louis University, Saint Louis, MO, 63104, USA
[b] Cardiovascular Group, Antisense Drug Discovery, Ionis Pharmaceuticals, Carlsbad, CA, 92010, USA
[c] Center for Cardiovascular Research, Saint Louis, MO, 63104, USA
[d] Liver Center, Saint Louis University, Saint Louis, MO, 63104, USA

ARTICLE INFO

Article history:
Received 27 March 2018
Received in revised form
8 May 2018
Accepted 23 May 2018
Available online 24 May 2018

Keywords:
FSP27
Atherosclerosis
Obesity
Hypertriglyceridemia
Antisense therapy

ABSTRACT

Background and aims: Obesity, hepatosteatosis, and hypertriglyceridemia are components of the metabolic syndrome and independent risk factors for cardiovascular disease. The lipid droplet-associated protein CIDEC (cell death-inducing DFFA-like effector C), known in mice as FSP27 (fat-specific protein 27), plays a key role in maintaining triacylglyceride (TAG) homeostasis in adipose tissue and liver, and controls circulating TAG levels in mice. Importantly, mutations and SNPs in *CIDEC* are associated with dyslipidemia and altered metabolic function in humans. Here we tested whether systemic silencing of *Fsp27* using antisense oligonucleotides (ASOs) was atheroprotective in LDL receptor knock-out (*Ldlr*$^{-/-}$) mice.

Methods: Atheroprone *Ldlr*$^{-/-}$ mice were fed a high-fat, high-cholesterol diet for 12 weeks while simultaneously dosed with saline, ASO-ctrl, or ASO-Fsp27.

Results: Data show that, compared to control treatments, silencing *Fsp27* significantly reduced body weight gain and visceral adiposity, prevented diet-induced hypertriglyceridemia, and reduced atherosclerotic lesion size both in *en face* aortas and in the aortic root.

Conclusions: Our findings suggest that therapeutic silencing of *Fsp27* with ASOs may be beneficial in the prevention and management of atherogenic disease in patients with metabolic syndrome.

1. Introduction

Central obesity, non-alcoholic fatty liver disease, insulin resistance, and hypertriglyceridemia are core manifestations of the metabolic syndrome (MetS) (reviewed in Ref. [1]). A global epidemic afflicting both adults and children, MetS is associated with increased risk for atherogenic cardiovascular disease, which ultimately leads to myocardial infarction and stroke. Although the mechanisms that link MetS and atherogenesis are yet to be fully elucidated, it was proposed that persistent systemic inflammation and dyslipidemia synergize to promote endothelial dysfunction, fatty streak formation, and other intimal perturbations in the arterial wall.

Lipid droplets (LDs) are critical organelles for intracellular metabolic regulation [2]. LD-associated proteins define the metabolic fate of the lipids stored within the LD. *CIDEC* (cell death-inducing DFF45-like effector C; referred to as *Fsp27* or fat specific protein 27 in mice) was originally identified as an abundant transcript in white and brown adipocytes [3], where it facilitates LD growth by both promoting LD fusion and inhibiting the action of lipases [4–7]. Two *CIDEC/Fsp27* isoforms (α and β) that differ in 10 aa at the N-terminus are expressed via alternative promoters [8]. *CIDEC/Fsp27* is barely detectable in the normal liver, but its expression is drastically elevated in the livers of obese patients [8–10] and mice [11–14], as well as in response to fasting in mice [11,15]. Recent studies showed that FSP27 activity modulates different physiological responses related to MetS. *Fsp27*$^{-/-}$ mice are lean, resistant to diet-induced obesity, and show enhanced insulin sensitivity [16,17]. Paradoxically, though, high-fat diet-fed *Fsp27*$^{-/-}$

Abbreviations: ASO, antisense oligonucleotide; CVD, cardiovascular disease; CIDEC, cell death-inducing DFFA-like effector C; FSP27, fat-specific protein 27; gWAT, gonadal white adipose tissue; HDL, high-density lipoprotein; HFD, high-fat diet; LD, lipid droplet; LDL, low-density lipoprotein; MetS, metabolic syndrome; NASH, non-alcoholic steatohepatitis; PPAR, peroxisome proliferator-activated receptor; TAG, triacylglyceride; VLDL, very low-density lipoprotein; WD, western diet.

* Corresponding author. Doisy Research Center, Saint Louis University, Room 615, Saint Louis, MO, 63104, USA.
E-mail address: angel.baldan@health.slu.edu (Á. Baldán).

https://doi.org/10.1016/j.atherosclerosis.2018.05.045

[18], *ob/ob* × *Fsp27*$^{-/-}$ [18], and adipocyte-specific *Fsp27*$^{-/-}$ [19] mice develop severe lipodystrophy, fatty liver, and insulin resistance. On the other hand, antisense oligonucleotide (ASO)-mediated silencing of *Fsp27* in genetic or dietary murine models of obesity and diabetes results in decreased visceral adiposity, reduced triacylglyceride (TAG) contents in fat pads, multilocular brown-like white adipocytes, reduced circulating VLDL-TAG, and improved whole-body glycemic control and multi-organ insulin sensitivity [12,20]. Acute shRNA-mediated knock-down of hepatic *Fsp27* reduces fasting and diet-induced hepatosteatosis [11,14,21]. In contrast, long-term systemic ASO-mediated *Fsp27* silencing abolishes diet-induced hepatic TAG accumulation only when used in combination with a fibrate [20], but not by itself [12,20]. Collectively, these reports suggest that silencing *Fsp27* may provide atheroprotection by ameliorating several independent cardiovascular risk factors. Herein we tested the effects of ASO-based anti-Fsp27 therapy on the progression of arterial disease in high fat, high cholesterol-fed atheroprone *Ldlr*$^{-/-}$ mice.

2. Materials and methods

2.1. Chemicals

Chimeric 2′-methoxyethyl control (5′-CCTTCCCTGAAGGTTCCTCC) and anti-Fsp27 (5′-CAGACTCTAATACCATTCAC) antisense oligonucleotides (ASOs) were synthesized and purified as described [22], suspended in saline, and stored at −20 °C until use.

2.2. Mouse studies

All animals were maintained in a 12 h/12 h light/dark cycle with *ad libitum* access to food and water. LDL-receptor knockout (*Ldlr*$^{-/-}$) mice (Jackson Laboratories stock 002207) were bred in our facility and kept on a normal diet (PicoLab Rodent Diet 20). At 12 weeks of age, male mice were switched to a western diet (WD) containing 21% fat and 1.25% cholesterol (Research Diets D12108) for 12 weeks. While on WD, 100 μL ASOs (25 mg/kg) or saline were injected *i. p.* twice weekly (Monday and Thursday). Mice were sacrificed at 9–10 a.m. without prior fasting, and plasma, liver, and gonadal white adipose tissue (gWAT), were harvested for analysis. In a subset of mice within each experimental group, resident macrophages were collected from peritoneal lavages. Studies were conducted in conformity with the Public Health Service policy on humane care and use of laboratory animals, and approved by the IACUC at Saint Louis University.

2.3. Plasma analysis

Blood samples were collected one week prior to start of WD and treatment regimen via superficial temporal vein bleeds, and upon sacrifice via inferior vena cava. Total cholesterol and triglycerides were assayed enzymatically using colorimetric kits (Wako Chemicals, Richmond, VA). Lipoprotein profiles were obtained by a modified Column Lipoprotein Profile (CLiP) method [23]. Briefly, 20 μL of pooled plasma were diluted in 60 μL of saline, and 40 μL of this mixture was auto-injected into a Superose-6 column (GE Healthcare, Wilmington, MA) using elution buffer (saline, 2 mmol/L EDTA, pH 7.4) at a flow rate of 0.6 mL/min at 40 °C. The eluate was immediately mixed with cholesterol or triglyceride reagent (Pointe Scientific, Ann Arbor, MI) at a flow rate of 0.2 mL/min, and incubated at 40 °C in a 5 m KOT coiled reactor. The final mixture entered a capillary spectrophotometric detector set at 500 nm, and the profiles were collected in real time using LC Solution software (Shimadzu, Kyoto, Japan).

2.4. Tissue lipid analysis

Lipids were extracted into chloroform by a modified Folch method [24], solubilized in water, and quantitated enzymatically using kits for triglycerides, total cholesterol, and FFAs (Wako Chemicals). Results were normalized to protein.

2.5. RNA analysis

RNA was isolated from tissues using Direct-zol RNA miniprep kit (ZYMO Research, Irvine, CA), and analyzed by real-time quantitative PCR using PowerSybrGreen (Life Technologies, Carlsbad, CA) and a LightCycler LC480 instrument (Roche, Indianapolis, IN). Values were normalized to *36b4*, and relative expression calculated using the $\Delta\Delta C_t$ method. Primer sequences are available upon request.

2.6. Histology

Samples of livers and gWAT were fixed in 10% formalin and embedded in paraffin blocks. Sections (5 μm) were processed for hematoxylin and eosin staining using standard techniques.

2.7. Analysis of atherosclerotic lesions

Whole aortas were dissected from the heart to the iliac bifurcation. Aortas and the upper half of the hearts were fixed in formalin-sucrose buffer (10% formalin, 20 μmol/L EDTA, 5% sucrose, pH 7.4), and stored at 4 °C. *En face* preparations of the aorta were pinned and stained with oil red O. Hearts were embedded in paraffin, and 20 serial sections (5 μm) of the aortic root (covering 1 mm around the aortic valve) were stained with hematoxylin and eosin. Atheromata were quantified using ImageJ software by a single operator blind to the identity of the samples, as described [25]. Select sections of the aortic root were stained with a monoclonal rat anti-mouse CD68 antibody (1:400 dilution; AbD Serotec) or Masson's trichrome to visualize macrophage and collagen content, respectively.

2.8. Macrophage studies

Macrophages from saline- and ASO-treated mice ($n = 5$ each) were isolated from the peritoneal cavity 4 days after injection of 2 mL of 3% thioglycollate broth. Red blood cells were removed with ACK lysis buffer (150 mmol/L NH_4Cl, 10 mmol/L $KHCO_3$, 0.1 mmol/L EDTA, pH 7.4), and pellets frozen for RNA extraction. Bone marrow cells were obtained from the tibias and femurs of chow-fed C57BL/6 mice, and differentiated to macrophages in media supplemented with 20 ng/mL M-CSF for 4 days, as described [26]. Cells were then incubated in media supplemented with PBS or 40 μg/mL oxLDL (AlfaAesar, Tewksbury, MA) overnight.

2.9. Statistical analysis

Data are shown as mean ± s. e.m. Differences between groups were analyzed by one-way ANOVA followed by post-hoc Bonferroni's test, using SPSS version 20.0 (IBM, Armonk, NY). Differences were considered significant at $p \leq 0.05$.

3. Results

To test the usefulness of therapeutic silencing of *Fsp27* on atherogenesis, male *Ldlr*$^{-/-}$ mice were fed a western diet for 12 weeks, while dosed with saline, ASO-control, or ASO-Fsp27. Fig. 1A and B show that treatment with ASO-Fsp27 reduced body weight

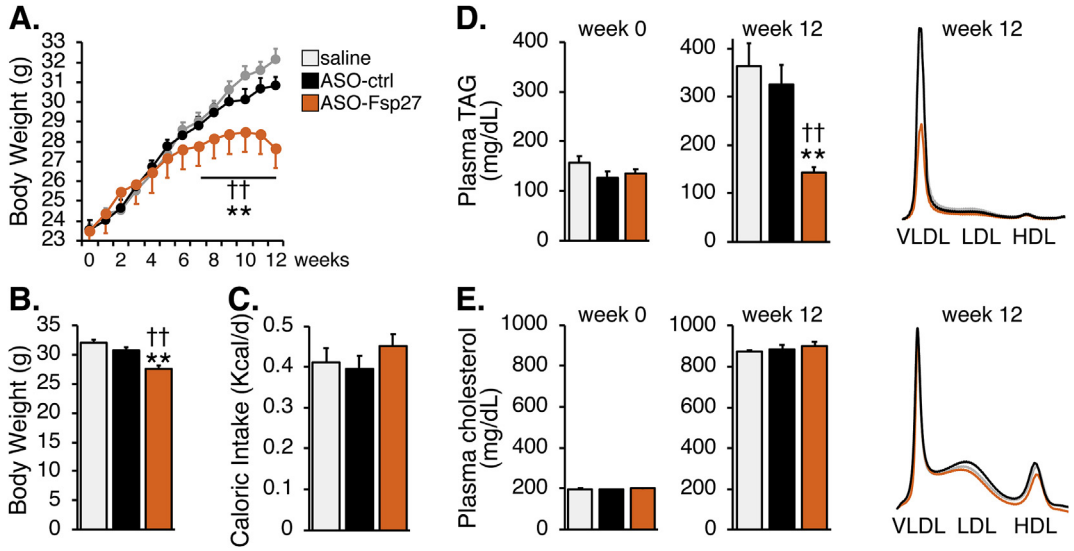

Fig. 1. ASO-Fsp27 therapy ameliorates diet-induced obesity and hypertriglyceridemia. *Ldlr*$^{-/-}$ mice were fed a WD for 12 weeks while injected twice weekly with saline, ASO-ctrl, or ASO-Fsp27.
(A) Weekly body weight gain. (B) Final body weight. (C) Caloric intake during the last week of the experiment. (D and E) Plasma lipid contents on weeks 0 and 12, and FPLC lipoprotein profiles on week 12. Data are shown as means ± s.e.m. ($n = 14$). *$p \leq 0.05$, **$p \leq 0.01$, compared to saline; ‡$p \leq 0.05$, ‡‡$p \leq 0.01$ compared to ASO-ctrl.

gain after 5 weeks, and led to a ~4 g reduction in body mass at the end of the 12-week feeding, compared to control mice. These changes occurred in the absence of significant differences in caloric intake (Fig. 1C). Analysis of plasma lipids in Fig. 1D–E revealed the expected diet-induced increase in TAG and cholesterol; however, treatment with ASO-Fsp27 resulted in a significant drop in VLDL-TAG. In contrast, no changes were observed in circulating cholesterol lipoprotein fractions.

The effects of ASO-Fsp27 therapy on body weight are likely due to the reduction in visceral adiposity (Fig. 2A and B). Unexpectedly, ASO-ctrl modestly reduced gonadal fat pad mass, compared to saline. Fig. 2D shows that *Fsp27* expression in epididymal white adipose tissue (eWAT) was efficiently and selectively silenced by ASO-Fsp27. Consistent with the data on tissue mass, eWAT TAG contents were reduced in ASO-treated mice, compared to saline; the effect of ASO-Fsp27, however, was considerably larger than that of ASO-ctrl (Fig. 2C). No changes were noted in tissue cholesterol contents. At the histological level, adipocytes in both the saline and ASO-ctrl groups appeared enlarged (Fig. 2E). In contrast, adipocytes from ASO-Fsp27-treated mice were smaller and heterogeneous, and ~10% of the cells were multilocular (Fig. 2E). Both the multilocular adipocytes and the large induction of *Ucp1*, *Dio2*, *Cox4*, and *Cidea* transcripts, compared to saline and ASO-ctrl groups (Fig. 2F), are consistent with a *browning* phenotype in response to *Fsp27* silencing. The elevated expression of lipolytic *Atgl* and *Hsl* transcripts in the same ASO-Fsp27 samples (Supplementary Fig. 1A) is also indicative of increased oxidative capacity, which is generally associated to these brown adipocyte-like adipocytes and likely accounts for the reduction in gonadal fat pad mass.

Fig. 3 shows that treatment with ASO-Fsp27 resulted in a slight enlargement of the liver, compared to the control groups. The reason for this is unknown, but it might reflect elevated water or glycogen contents. As expected, ASO-Fsp27 silenced Fsp27 expression by ~90%, compared to saline. Unexpectedly, ASO-ctrl also reduced, albeit modestly, the expression of *Fsp27*, compared to saline. TAG contents were similarly reduced in mice injected with ASO-ctrl or ASO-Fsp27, compared to saline. No differences in hepatic cholesterol contents were found among groups. Consistent with changes in TAG contents, histological analysis revealed large areas of macrovesicular steatosis in the saline group, which were absent in the slightly darker livers from mice injected with either ASO. Similar to eWAT, loss of *Fsp27* expression resulted in a compensatory increase in *Cidea* mRNA. The expression of transcripts encoding other hepatic lipid droplet-associated proteins (*Plin2*, *Plin5*) was reduced by either ASO, compared to saline, likely a consequence of reduced tissue lipid contents; however, no major differences were noted comparing ASO-ctrl and ASO-Fsp27 treatments. Additionally, the expression of *Atgl* and *Hsl* was reduced and induced, respectively, in ASO-treated mice compared to saline, but no differences were noted between ASO treatment groups (Supplementary Fig. 1B). In contrast to WAT, the expression of *Angptl* transcripts remained unchanged among groups (Supplementary Fig. 1B). Overall, major differences among groups in both hepatic TAG content and mRNA profiles were largely mediated by oligonucleotide delivery, independent on silencing *Fsp27*.

Finally, analysis of atherosclerotic lesions both in *en face* preparations of the aorta (Fig. 4A) and in the aortic root (Fig. 4B) revealed a significant reduction in lesion size in the ASO-Fsp27 group, compared to saline and ASO-ctrl groups. CD68^{+} macrophage contents and collagen staining were increased in the roots of ASO-Fsp27–treated mice, compared to saline or ASO-ctrl (Fig. 4B); in contrast, necrotic core areas were smaller in the ASO-Fsp27 group, compared with control animals. These latter results are consistent with less advanced lesions in the ASO-Fsp27–treated mice. Collectively, the data suggest a potent atheroprotective effect following silencing of *Fsp27*. Since we used only male mice in this study, additional experiments are needed to establish whether the atheroprotection extends to female animals.

A potential explanation for the reduced lesion size in ASO-Fsp27-treated mice could be that silencing *Fsp27* expression in macrophages impairing cholesterol loading and thus limits the development of the initial fatty streak in the subendothelial space. To test this hypothesis, we harvested macrophages from peritoneal lavages in a subset of *Ldlr*$^{-/-}$ mice used above, and from an additional group of chow-fed (and thus, only mildly hypercholesterolemic) *Ldlr*$^{-/-}$ animals (Supplementary Fig. 2A). Representative photographs of oil red O-stained cells show that cells from WD-fed

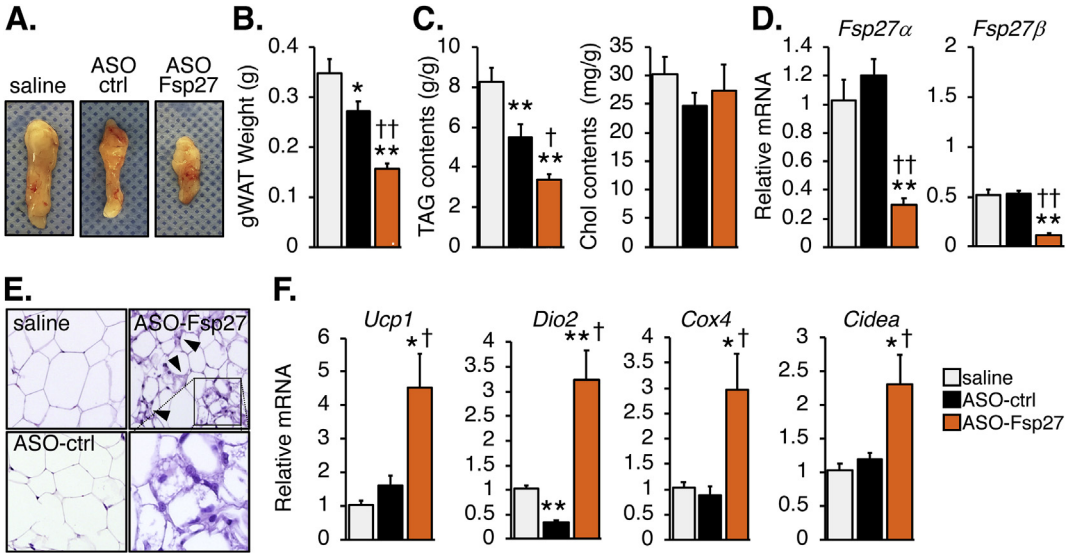

Fig. 2. ASO-Fsp27 induces browning of gonadal adipose tissue.
(A) Representative macroscopic appearance of left gonadal fat pads in each experimental group. (B) Average tissue weight. (C) Relative lipid contents, normalized to protein contents. (D) Relative expression of *Fsp27*. (E) Representative micrographs of hematoxylin and eosin-stained sections. Scale bars represent 50 μm. Arrows indicate multilocular cells. Insert is magnified to show brown-like adipocytes. (F) Relative mRNA expression of thermogenesis/browning markers in the same samples. Data are shown as means ± s.e.m. ($n = 14$ for panel B; $n = 6$ for panels C, D, and F). $^{*}p \leq 0.05$, $^{**}p \leq 0.01$, compared to saline; $^{\dagger}p \leq 0.05$, $^{\dagger\dagger}p \leq 0.01$ compared to ASO-ctrl.

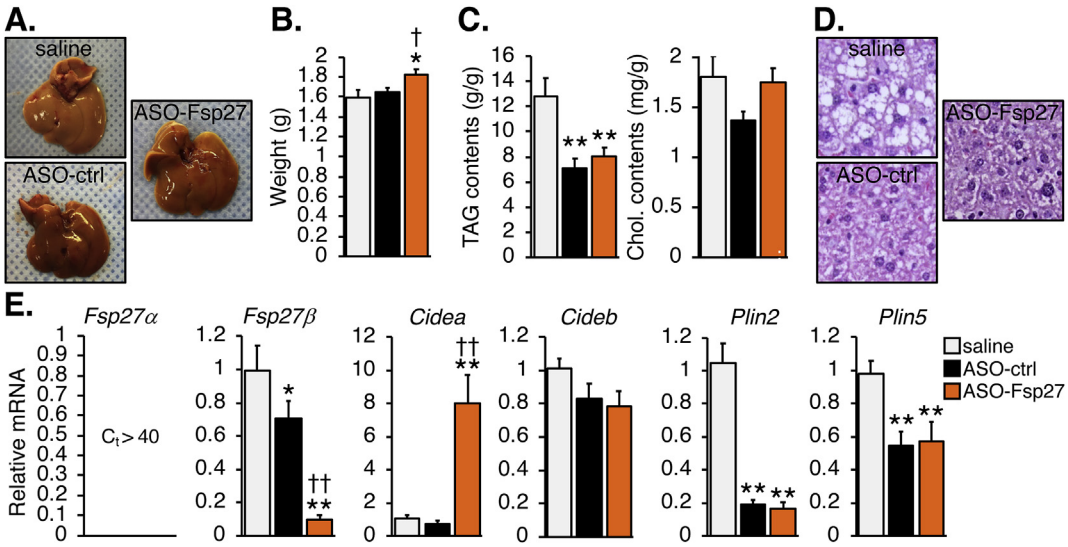

Fig. 3. ASO-Fsp27 does not impact hepatic steatosis.
(A) Representative macroscopic appearance of the livers in each experimental group. (B) Average liver weight. (C) Relative lipid contents, normalized to protein. (D) Representative micrographs of hematoxylin and eosin-stained sections. Scale bars represent 50 μm. (E) Relative mRNA expression of *Fsp27* and other transcripts encoding LD-associated proteins. Data are shown as means ± s.e.m. ($n = 14$ for panel B; $n = 6$ for panels C and E). $^{*}p \leq 0.05$, $^{**}p \leq 0.01$, compared to saline; $^{\dagger}p \leq 0.05$, $^{\dagger\dagger}p \leq 0.01$ compared to ASO-ctrl.

mice had more lipid droplets than those collected from chow-fed animals, but the variation in the numbers and size of intracellular lipid droplet was similar among the 3 WD-fed groups. Data show that *Fsp27* is actually not expressed in these macrophages ($C_t > 40$ when using primers for either the α or β isoforms), independent on cholesterol loading. As anticipated, canonical LXR targets (*Abca1* and *Abcg1*) and SREBP2 targets (*Hmgcr, Sqs*) were induced and repressed, respectively, in cells recovered from WD-fed mice, compared to those from chow-fed animals, but no differences in the levels of these transcripts were noted in cells from ASO-Fsp27–treated mice, compared to saline or ASO-ctrl (Supplementary Fig. 2A). Analysis of selected transcripts suggests that these peritoneal macrophages were predominantly M2-like cells (high *Arg1* and *Tgfβ*; low *Tnfα* and *Il6*), and that ASO-Fsp27 did not affect macrophage polarization (Supplementary Fig. 2A). To further establish whether the expression of *Fsp27* is modulated during foam cell formation, we cultured murine bone marrow-derived macrophages in the absence or presence of oxidized LDL (oxLDL) (Supplementary Fig. 2B). As expected, the expression of LXR and SREBP2 targets was increased and decreased, respectively, in response to oxLDL treatment. Data show that *Fsp27* is again undetectable in these cells, independent on cholesterol loading. Taken together, the results in Supplementary Fig. 2 demonstrate that *Fsp27* is absent in the murine macrophage, and strongly suggest that FSP27 activity does not play a role on lipid droplet growth during macrophage foam cell conversion in the early stages of atherogenesis.

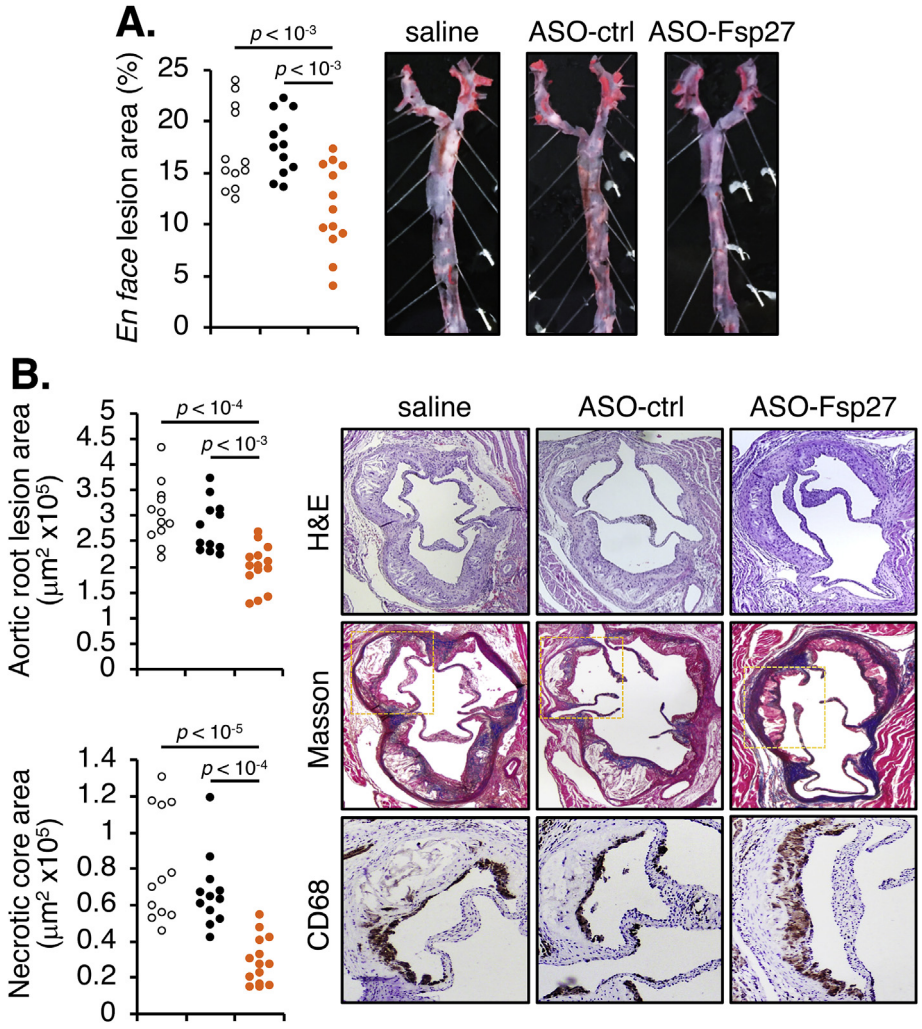

Fig. 4. ASO-Fsp27 attenuates the progression of atherosclerosis.
(A) Lesion size in oil red O-stained *en face* preparations of the aortas, and representative images for each experimental group. (B) Left panel, total atheroma size and necrotic core size in the aortic root. Right panel, representative micrographs of serial sections stained with hematoxylin and eosin (H&E), Masson trichrome (collagen deposition in blue), and CD68 for macrophages (area corresponding to yellow rectangle in Masson panel; CD68 signal is dark brown). In both panels, each dot denotes a single animal.

4. Discussion

The role of FSP27 on adipocyte TAG metabolism has been firmly established. Biochemical studies showed that FSP27 dimerizes and mediates the fusion of small LDs and the transfer of lipids between them [27,28]. Other studies suggested that FSP27 also physically interacts with and inhibits the activity of lipases at the surface of the LD [29]. The overall result is that FSP27 activity promotes the expansion and growth of LDs. Whole-body [16–18] and adipocyte-specific [19] *Fsp27*$^{-/-}$ mice show a lipodystrophy-like phenotype with multilocular white adipocytes that validates the biochemical studies. Our studies using *i.p.* injected ASOs in chow-fed *ob/ob* [12], HFD-fed C57BL/6 [12], NASH-fed C57BL/6 [20], and *Ldlr*$^{-/-}$ (herein) mice have consistently shown reduced visceral adiposity following silencing *Fsp27*, but not lipodystrophy. Importantly, we report here that ASOs *per se,* independent on changes in *Fsp27* expression, markedly reduced eWAT and liver TAG contents, compared to saline treatment. The reduction in hepatic TAG contents following injection of 2′-methoxyethyl oligonucleotides is known in the field, although the mechanism remains unknown. Hence, most published studies have focused only on changes compared to ASO-ctrl. In our hands, ASO-ctrl induced specific changes in the expression of several lipid-related genes in eWAT and liver, compared to saline, which likely explain the reduced TAG contents in these tissues. Consistent with our previous ASO studies, here we report that therapeutic silencing of *Fsp27* further reduces eWAT size and TAG contents but has no effect on liver hepatosteatosis, compared to ASO-ctrl.

In the liver, CIDEC/FSP27 expression is strongly linked to TAG accumulation, both in patients [8–10] and in mice [11–14]. The functional consequences of loss of hepatic *Fsp27* function are controversial, though. Acute knockdown of *Fsp27* in the liver via adenoviral-mediated shRNA ameliorates fasting- [11] and diet-[11,14,21] induced steatosis. In contrast, long-term silencing of *Fsp27* via ASOs has no effect on hepatic TAG content in mouse models of obesity, diabetes, and fatty liver [12,20]. However, diet-induced murine hepatosteatosis is synergistically reduced when ASO-Fsp27 and fenofibrate (a PPARα synthetic agonist which does not reduce hepatic TAG contents by itself) are combined [20]. Metabolic labeling experiments in primary hepatocytes in culture demonstrated that *Fsp27* activity reduces TAG turnover in the LD, and that efficient mitochondrial oxidation of fatty acids requires simultaneous *Fsp27* knock-down and PPARα activation [11], nicely recapitulating the *in vivo* data [20].

Accelerated secretion of VLDL particles is a fundamental property of atherogenic dyslipidemia, which ultimately results in elevated numbers of atherogenic VLDL remnants and LDL particles [30,31]. Hence, hypertriglyceridemia has been identified as an independent risk factor for atherogenic cardiovascular disease, and it was proposed that cholesterol-rich VLDL-remnant particles generated by lipases in peripheral tissues can infiltrate the arterial sub-endothelial space and contribute to atherogenesis. Our data in previous reports [11,12,20] and herein suggest that hepatic FSP27 activity promotes VLDL-TAG secretion. Importantly, two SNPs in *CIDEC* are associated to elevated fasting triglyceridemia [32]. We hypothesize that the large reduction in circulating VLDL-TAG in ASO-Fsp27-treated mice is, at least in part, a driver for the atheroprotective phenotype in our study by limiting the availability of remnant particles. Importantly, despite both ASO-ctrl and ASO-Fsp27 treatments reduced hepatic TAG contents, the reduction in both plasma VLDL-TAG and atherosclerotic lesions were confined solely to the ASO-Fsp27–treated group; no significant differences in circulating lipids or atheromata were noted between the saline and ASO-ctrl groups. Additional experiments are currently in place to determine how FSP27 activity regulates VLDL maturation, secretion, or clearance. Interestingly, lipid lowering has been shown to increase collagen deposition and promote stability of atheromata by reducing the expression of matrix-degrading enzymes in lesional macrophages [33,34]. Our data showing reduced plasma lipids and increased collagen contents in the aortic roots of ASO-Fsp27-treted mice are consistent with this idea.

Cholesterol-laden foam cells in fatty streaks express various lipid droplet-associated proteins that promote pro- or anti-atherogenic phenotypes (reviewed in Ref. [35]). For example, loss of bone marrow-derived *Plin1* [36] or *Plin2* [37] expression results in reduced foam cell conversion and is atheroprotective in *ApoE*$^{-/-}$ mice. Notably, the changes in aortic lesion size in our study cannot be attributable to a role of FSP27 on foam cell formation. Indeed, we show that *Fsp27* is essentially not expressed in cholesteryl esters-loaded peritoneal macrophages recovered from the *Ldlr*$^{-/-}$ mice. Additionally, *Fsp27* expression is not induced following lipid loading with oxLDL in bone marrow-derived macrophages. Overall, these data suggest that the decrease in lesion size in the arterial wall in response to ASO-Fsp27 treatment is likely secondary to the availability of atherogenic mediators, rather than a defect in foam cell conversion.

Our results also underline the different outcomes of genetic (*i.e.*, knock-out) and interventional (*i.e.*, ASO) mouse models. Thus, the phenotype in high-fat diet-fed ASO-Fsp27–treated mice (reduced adiposity, no deleterious effects in liver, hypotriglyceridemia, enhanced insulin sensitivity in gWAT, liver, and muscle, and improved whole-body glycemic control) [12,20] sharply differs from that in high-fat diet-fed *Fsp27*$^{-/-}$ [18], *ob/ob* × *Fsp27*$^{-/-}$ [18], or adipocyte-specific *Fsp27*$^{-/-}$ [19] mice (lipodystrophy, fatty liver, hypertriglyceridemia, insulin resistance). We posit that the latter outcomes are secondary to the severe lipodystrophy in *Fsp27*$^{-/-}$ mice and subsequent ectopic liver lipid deposition. Residual *Fsp27* activity in WAT, independent on dietary overload, likely prevents lipodystrophy and its consequences in ASO-Fsp27–treated mice. Further experiments where ASO-Fsp27 is administered for longer periods of time, though, are needed to verify that a prolonged reduction in visceral fat does not have deleterious consequences on liver function, and whole-body insulin sensitivity and glycemic control. It will also be important to establish whether sustained silencing of *Fsp27* impacts the inflammatory state of the mice. Reduced systemic inflammation resulting from improved lipid homeostasis in liver and/or WAT might be an additional contributing mechanism for ASO-Fsp27–driven atheroprotection. Finally, whether therapeutic silencing of FSP27 can not only attenuate the progression of new plaques, but also promote the regression of pre-established atheromata remains to be established.

Lifestyle modifications that include improved diet, increased physical activity, and smoking and alcohol cessation, have long been established as beneficial for CVD patients [38]. The arsenal of pharmaceutical agents for these patients include anti-hypertensive, anti-thrombotic, and lipid-lowering drugs. Yet, despite these therapeutic tools, atherosclerotic CVD and its complications remain a major cause of death globally. Taken together, our data in this and previous reports suggest that, due its multifactorial beneficial effects on cardiovascular risk factors that include visceral adiposity, hepatosteatosis, glucose homeostasis, and hypertriglyceridemia, CIDEC/FSP27 may be exploited therapeutically in patients with metabolic syndrome who are at increased risk of atherosclerotic CVD.

In summary, this is the first report on the consequences of therapeutic silencing of *Fsp27* on atherogenesis. Our data demonstrate that ASO-Fsp27 reduces diet-induced visceral obesity, circulating VLDL-TAG, and atheromata in *Ldlr*$^{-/-}$ mice. We also show that *Fsp27* is not expressed in macrophages, which suggests that atheroprotection is not mediated by direct effects of ASO-Fsp27 on foam cell conversion in the plaque.

Conflicts of interest

A.R. and Á.B. declare no competing financial interests. R.G.L. is an employee and shareholder of Ionis Pharmaceuticals, Inc.

Financial support

This study was supported in part by NIH grant HL107794 and intramural PRF grant 9109 (to Á.B.) and an American Heart Association Clinical Health Profession Student Training Program fellowship 17CPRE33670519 (to A.R.).

Author contributions

A.R. and Á.B. conceived and designed the study, and wrote the manuscript. A.R. performed the study and analyzed the data. R.G.L. provided the antisense oligonucleotides. All authors approved the manuscript.

Acknowledgements

We thank Grant Kolar and Barbara Nagel at the Research Microscopy and Histology Core at Saint Louis University for excellent technical support. We also thank Dr. Noemi Arias in the Baldan lab and the members of the Cardiovascular Research Center and the Liver Center at Saint Louis University for helpful discussions. Á.B. dedicates this paper to Bender (2010–2018): fly forever free, write songs across the sky.

Appendix A. Supplementary data

Supplementary data related to this article can be found at https://doi.org/10.1016/j.atherosclerosis.2018.05.045.

References

[1] K.G. Alberti, R.H. Eckel, S.M. Grundy, P.Z. Zimmet, J.I. Cleeman, K.A. Donato, et al., Harmonizing the metabolic syndrome: a joint interim statement of the international diabetes federation task force on epidemiology and prevention; national heart, lung, and blood institute; american heart association; world heart federation; international atherosclerosis society; and international association for the study of obesity, Circulation 120 (16) (2009) 1640–1645.
[2] T.C. Walther, R.V. Farese Jr., Lipid droplets and cellular lipid metabolism, Annu.

Rev. Biochem. 81 (2012) 687–714.
[3] U. Danesch, W. Hoeck, G.M. Ringold, Cloning and transcriptional regulation of a novel adipocyte-specific gene, FSP27. CAAT-enhancer-binding protein (C/EBP) and C/EBP-like proteins interact with sequences required for differentiation-dependent expression, J. Biol. Chem. 267 (10) (1992) 7185–7193.
[4] P. Keller, J.T. Petrie, P. De Rose, I. Gerin, W.S. Wright, S.H. Chiang, et al., Fat-specific protein 27 regulates storage of triacylglycerol, J. Biol. Chem. 283 (21) (2008) 14355–14365.
[5] J. Gong, Z. Sun, L. Wu, W. Xu, N. Schieber, D. Xu, et al., Fsp27 promotes lipid droplet growth by lipid exchange and transfer at lipid droplet contact sites, J. Cell Biol. 195 (6) (2011) 953–963.
[6] L. Xu, L. Zhou, P. Li, CIDE proteins and lipid metabolism, Arterioscler. Thromb. Vasc. Biol. 32 (5) (2012) 1094–1098.
[7] V. Puri, S. Konda, S. Ranjit, M. Aouadi, A. Chawla, M. Chouinard, et al., Fat-specific protein 27, a novel lipid droplet protein that enhances triglyceride storage, J. Biol. Chem. 282 (47) (2007) 34213–34218.
[8] X. Xu, J.G. Park, J.S. So, A.H. Lee, Transcriptional activation of Fsp27 by the liver-enriched transcription factor CREBH promotes lipid droplet growth and hepatic steatosis, Hepatology 61 (3) (2015) 857–869.
[9] A.M. Hall, E.M. Brunt, S. Klein, B.N. Finck, Hepatic expression of cell death-inducing DFFA-like effector C in obese subjects is reduced by marked weight loss, Obesity 18 (2) (2010) 417–419.
[10] M.J. Xu, Y. Cai, H. Wang, J. Altamirano, B. Chang, A. Bertola, et al., Fat-specific protein 27/CIDEC promotes development of alcoholic steatohepatitis in mice and humans, Gastroenterology 149 (4) (2015) 1030–1041 e1036.
[11] C. Langhi, A. Baldan, CIDEC/FSP27 is regulated by peroxisome proliferator-activated receptor alpha and plays a critical role in fasting- and diet-induced hepatosteatosis, Hepatology 61 (4) (2015) 1227–1238.
[12] C. Langhi, N. Arias, A. Rajamoorthi, J. Basta, R.G. Lee, A. Baldan, Therapeutic silencing of fat-specific protein 27 improves glycemic control in mouse models of obesity and insulin resistance, J. Lipid Res. 58 (1) (2017) 81–91.
[13] S. Yu, K. Matsusue, P. Kashireddy, W.Q. Cao, V. Yeldandi, A.V. Yeldandi, et al., Adipocyte-specific gene expression and adipogenic steatosis in the mouse liver due to peroxisome proliferator-activated receptor gamma1 (PPARgamma1) overexpression, J. Biol. Chem. 278 (1) (2003) 498–505.
[14] K. Matsusue, T. Kusakabe, T. Noguchi, S. Takiguchi, T. Suzuki, S. Yamano, et al., Hepatic steatosis in leptin-deficient mice is promoted by the PPARgamma target gene Fsp27, Cell Metabol. 7 (4) (2008) 302–311.
[15] A. Vila-Brau, A.L. De Sousa-Coelho, J.F. Goncalves, D. Haro, P.F. Marrero, Fsp27/CIDEC is a CREB target gene induced during early fasting in liver and regulated by FA oxidation rate, J. Lipid Res. 54 (3) (2013) 592–601.
[16] N. Nishino, Y. Tamori, S. Tateya, T. Kawaguchi, T. Shibakusa, W. Mizunoya, et al., FSP27 contributes to efficient energy storage in murine white adipocytes by promoting the formation of unilocular lipid droplets, J. Clin. Invest. 118 (8) (2008) 2808–2821.
[17] S.Y. Toh, J. Gong, G. Du, J.Z. Li, S. Yang, J. Ye, et al., Up-regulation of mitochondrial activity and acquirement of brown adipose tissue-like property in the white adipose tissue of fsp27 deficient mice, PLoS One 3 (8) (2008) e2890.
[18] L. Zhou, S.Y. Park, L. Xu, X. Xia, J. Ye, L. Su, et al., Insulin resistance and white adipose tissue inflammation are uncoupled in energetically challenged Fsp27-deficient mice, Nat. Commun. 6 (5949) (2015).
[19] N. Tanaka, S. Takahashi, T. Matsubara, C. Jiang, W. Sakamoto, T. Chanturiya, et al., Adipocyte-specific disruption of fat-specific protein 27 causes hepatosteatosis and insulin resistance in high-fat diet-fed mice, J. Biol. Chem. 290 (5) (2015) 3092–3105.
[20] A. Rajamoorthi, N. Arias, J. Basta, R.G. Lee, A. Baldan, Amelioration of diet-induced steatohepatitis in mice following combined therapy with ASO-Fsp27 and fenofibrate, J. Lipid Res. 58 (11) (2017) 2127–2138.
[21] W. Wang, M.J. Xu, Y. Cai, Z. Zhou, H. Cao, P. Mukhopadhyay, et al., Inflammation is independent of steatosis in a murine model of steatohepatitis, Hepatology 66 (1) (2017) 108–123.
[22] P.P. Seth, G. Vasquez, C.A. Allerson, A. Berdeja, H. Gaus, G.A. Kinberger, et al., Synthesis and biophysical evaluation of 2',4'-constrained 2'O-methoxyethyl and 2',4'-constrained 2'O-ethyl nucleic acid analogues, J. Org. Chem. 75 (5) (2010) 1569–1581.
[23] D.W. Garber, K.R. Kulkarni, G.M. Anantharamaiah, A sensitive and convenient method for lipoprotein profile analysis of individual mouse plasma samples, J. Lipid Res. 41 (6) (2000) 1020–1026.
[24] T.P. Carr, C.J. Andresen, L.L. Rudel, Enzymatic determination of triglyceride, free cholesterol, and total cholesterol in tissue lipid extracts, Clin. Biochem. 26 (1) (1993) 39–42.
[25] R.K. Tangirala, E.M. Rubin, W. Palinski, Quantitation of atherosclerosis in murine models: correlation between lesions in the aortic origin and in the entire aorta, and differences in the extent of lesions between sexes in LDL receptor-deficient and apolipoprotein E-deficient mice, J. Lipid Res. 36 (11) (1995) 2320–2328.
[26] X. Zhang, R. Goncalves, D.M. Mosser, The isolation and characterization of murine macrophages, Curr Protoc Immunol Chapter 14 (Unit 14 11) (2008).
[27] Z. Sun, J. Gong, H. Wu, W. Xu, L. Wu, D. Xu, et al., Perilipin1 promotes unilocular lipid droplet formation through the activation of Fsp27 in adipocytes, Nat. Commun. 4 (1594) (2013).
[28] T.H. Grahn, Y. Zhang, M.J. Lee, A.G. Sommer, G. Mostoslavsky, S.K. Fried, et al., FSP27 and PLIN1 interaction promotes the formation of large lipid droplets in human adipocytes, Biochem. Biophys. Res. Commun. 432 (2) (2013) 296–301.
[29] T.H. Grahn, R. Kaur, J. Yin, M. Schweiger, V.M. Sharma, M.J. Lee, et al., Fat-specific protein 27 (FSP27) interacts with adipose triglyceride lipase (ATGL) to regulate lipolysis and insulin sensitivity in human adipocytes, J. Biol. Chem. 289 (17) (2014) 12029–12039.
[30] M. Adiels, S.O. Olofsson, M.R. Taskinen, J. Boren, Overproduction of very low-density lipoproteins is the hallmark of the dyslipidemia in the metabolic syndrome, Arterioscler. Thromb. Vasc. Biol. 28 (7) (2008) 1225–1236.
[31] P.P. Toth, Triglyceride-rich lipoproteins as a causal factor for cardiovascular disease, Vasc. Health Risk Manag. (12) (2016) 171–183.
[32] H. Wang, Y. Ti, J.B. Zhang, J. Peng, H.M. Zhou, M. Zhong, et al., Single nucleotide polymorphisms in CIDEC gene are associated with metabolic syndrome components risks and antihypertensive drug efficacy, Oncotarget 8 (16) (2017) 27481–27488.
[33] M. Aikawa, E. Rabkin, Y. Okada, S.J. Voglic, S.K. Clinton, C.E. Brinckerhoff, et al., Lipid lowering by diet reduces matrix metalloproteinase activity and increases collagen content of rabbit atheroma: a potential mechanism of lesion stabilization, Circulation 97 (24) (1998) 2433–2444.
[34] Y. Fukumoto, P. Libby, E. Rabkin, C.C. Hill, M. Enomoto, Y. Hirouchi, et al., Statins alter smooth muscle cell accumulation and collagen content in established atheroma of watanabe heritable hyperlipidemic rabbits, Circulation 103 (7) (2001) 993–999.
[35] J. Plakkal Ayyappan, A. Paul, Y.H. Goo, Lipid droplet-associated proteins in atherosclerosis (Review), Mol. Med. Rep. 13 (6) (2016) 4527–4534.
[36] X. Zhao, M. Gao, J. He, L. Zou, Y. Lyu, L. Zhang, et al., Perilipin1 deficiency in whole body or bone marrow-derived cells attenuates lesions in atherosclerosis-prone mice, PLoS One 10 (4) (2015) e0123738.
[37] A. Paul, B.H. Chang, L. Li, V.K. Yechoor, L. Chan, Deficiency of adipose differentiation-related protein impairs foam cell formation and protects against atherosclerosis, Circ. Res. 102 (12) (2008) 1492–1501.
[38] K.N. Doughty, N.X. Del Pilar, A. Audette, D.L. Katz, Lifestyle medicine and the management of cardiovascular disease, Curr. Cardiol. Rep. 19 (11) (2017) 116.